AGU PUBLICATIONS

Geophysical Research Letters

RESEARCH LETTER
10.1002/2016GL068971

Key Points:
- AOGCMs overestimate long-term correlations in sea level fluctuations in the North Atlantic
- The NCAR CESM1-CAM5 historical run gives the best fit to observed sea level scaling
- CMIP5 AOGCMs can mask the part of sea level trend driven by external forcings

Supporting Information:
- Supporting Information S1
- Table S1
- Table S2
- Figure S1

Correspondence to:
M. Becker,
melanie.becker@ird.fr

Citation:
Becker, M., M. Karpytchev, M. Marcos, S. Jevrejeva, and S. Lennartz-Sassinek (2016), Do climate models reproduce complexity of observed sea level changes?, *Geophys. Res. Lett.*, *43*, 5176–5184, doi:10.1002/2016GL068971.

Received 11 FEB 2016
Accepted 29 APR 2016
Accepted article online 4 MAY 2016
Published online 18 MAY 2016

Do climate models reproduce complexity of observed sea level changes?

M. Becker[1,2], M. Karpytchev[3], M. Marcos[4], S. Jevrejeva[5], and S. Lennartz-Sassinek[6]

[1]LEGOS/IRD UMR 5566, Toulouse, France, [2]Now at LIENSs/CNRS UMR 7266, University of La Rochelle, France, [3]LIENSs/CNRS UMR 7266, University of La Rochelle, France, [4]IMEDEA(UIB-CSIC), Mallorca, Spain, [5]NOC, Liverpool, UK, [6]Institute for Geophysics and Meteorology, University of Cologne, Cologne, Germany

Abstract The ability of Atmosphere-Ocean General Circulation Models (AOGCMs) to capture the statistical behavior of sea level (SL) fluctuations has been assessed at the local scale. To do so, we have compared scaling behavior of the SL fluctuations simulated in the historical runs of 36 CMIP5 AOGCMs to that in the longest (>100 years) SL records from 23 tides gauges around the globe. The observed SL fluctuations are known to manifest a power law scaling. We have checked if the SL changes simulated in the AOGCM exhibit the same scaling properties and the long-term correlations as observed in the tide gauge records. We find that the majority of AOGCMs overestimates the scaling of SL fluctuations, particularly in the North Atlantic. Consequently, AOGCMs, routinely used to project regional SL rise, may underestimate the part of the externally driven SL rise, in particular the anthropogenic footprint, in the projections for the 21st century.

1. Introduction

Assessing the rate of current mean sea level rise (SLR) and projecting its future changes are issues of growing practical significance in climate studies given its broad impact on coastal regions. Globally, SLR is driven by changes of ocean water volume due to ocean-mass addition (land water, glaciers, and ice sheets), oceanic warming, and by the deformation of the solid Earth changing the shape of oceanic basins [*Mitchum et al.*, 2010]. At the regional scale, SLR can significantly differ from the global average not only on the short-term but also on the interannual to decadal time scales. This pronounced regional sea level variability is a consequence of changing ocean-atmosphere circulation as well as of local solid-Earth processes such as sediment compaction and tectonics [*Church et al.*, 2004; *Jevrejeva et al.*, 2006; *Cazenave and Llovel*, 2010; *Nerem et al.*, 2010; *Becker et al.*, 2012; *Stammer et al.*, 2013]. The diversity and complexity of processes driving regional SLR make it challenging to approach the understanding and projections of sea level in a comprehensive and coherent manner. The Atmosphere–Ocean General Circulation Models (AOGCMs) are one of the main tools currently used for forecasting SLR at global and regional scales. These models provide, on one hand, the "dynamical ocean component," i.e., changes in local sea surface heights (SSH) resulting from temperature and salinity variations and momentum fluxes and, on the other hand, the global mean of steric sea level change that must be added to SSH, as the AOGCMs are volume conserving models [*Griffies and Greatbatch*, 2012]. The Coupled Model Intercomparison Project (CMIP) under the World Climate Research Program undertakes regular intercomparisons of the AOGCM outputs. A reasonable approach for assessing the AOGCM performances is to compare the modeled SSH to observations from sea level stations and satellite altimetry. In comparing the AOGCM CMIP5 outputs to the available 20 year long satellite altimetry observations, *Landerer et al.* [2014] noticed that most CMIP5 models overestimated the observed standard deviation of SSH fluctuations; likewise, *Bilbao et al.* [2015] revealed regional inconsistencies between the AOGCMs and the altimetry data due to inadequate modeling of internal sea level variability. However, a period of only 20 years is too short for evaluating the AOGCM performance on a longer time scale. Alternatively, historical tide gauge (TG) records provide a unique set of sea level measurements over the past centuries. Comparing them with the AOGCMs outputs can therefore shed some light on the performance of models over a longer term, at decadal and centennial time scales.

Sea level fluctuations result from complex interactions between diverse physical processes and, as many other geophysical signals, exhibit long-term correlations (LTC), also called long-term memory or long-term persistence [*Agnew*, 1992], that can be effectively modeled as outcomes of stochastic power law process with a Hurst exponent $H > 0.5$ [*Beretta et al.*, 2005; *Barbosa et al.*, 2008; *Bos et al.*, 2013]. The Hurst exponent $0.5 < H < 1$ indicates the presence of LTC that manifest themselves as persistent low-frequency oscillations

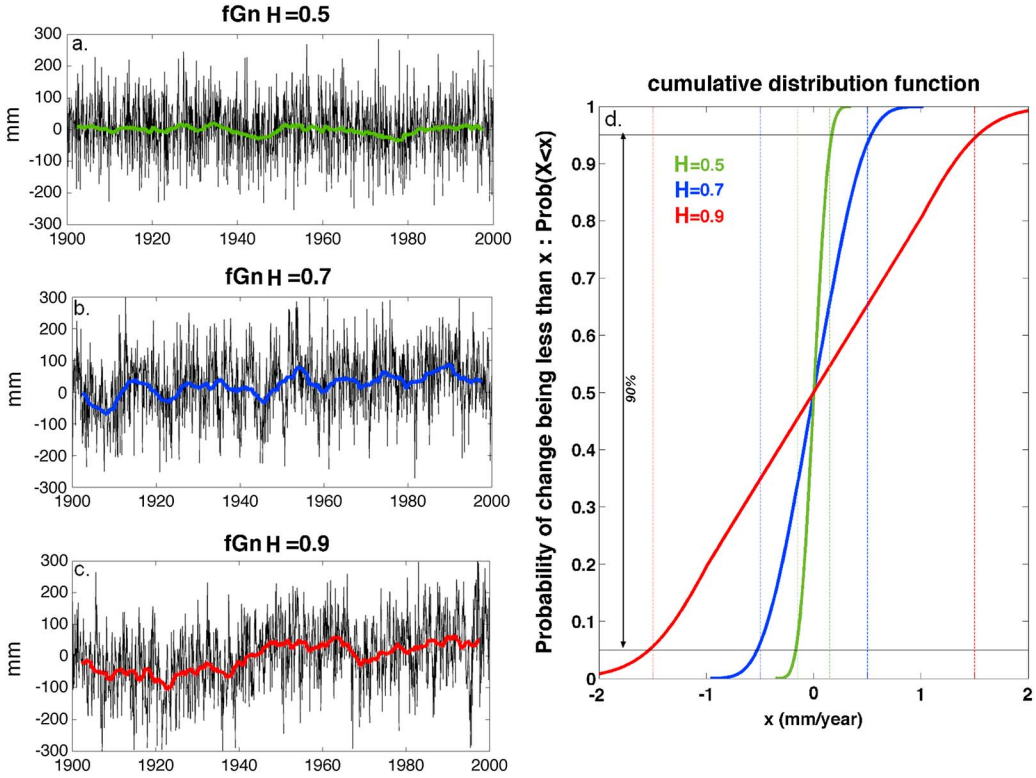

Figure 1. Schematic illustration of the long-term correlation (LTC) impact on sea level variability. (left) Centennial LTC time series (black line) of length 1200 months with a standard deviation of 100 mm and prescribed Hurst exponent *H*, obtained from fractional Gaussian noise (fGn) (a) $H = 0.5$ (uncorrelated), (b) $H = 0.7$ (LTC), and (c) $H = 0.9$ (LTC). The full line shows the moving average over 60 months. (right) Cumulative distribution function of 10000 surrogate data sets of centennial LTC time series trends with prescribed H.

[*Feder*, 1988; *Beran*, 1994; *Rybski and Bunde*, 2009]. The interplay of long-term correlated fluctuations results in a power law increase of sea level spectral energy toward low frequencies. This power law behavior is fundamental for realistic simulation of natural sea level variability, accurate modeling of energy distribution in the sea level spectrum, and for detecting an anthropogenic impact as well as for estimating uncertainties in the predicted sea level trends [*Hughes and Williams*, 2010]. In the LTC records, large events well above the average are more likely to be followed by large events and small events well below the average by small events [*Hurst et al.*, 1965; *Mandelbrot and Wallis*, 1968, 1969]. In other words, a period of a lowstand of the sea level is more likely to be followed by a low sea level, whereas a high sea level is more probably followed by a high one. These LTC hold, in theory, on over all time scales and may look like positive or negative trends in the sea level data. To illustrate this point we show in Figure 1 an uncorrelated (Figure 1a) and two long-term correlated 1200 month times series. For the uncorrelated data (Figure 1a), the moving average (full bold line) is close to zero, while for the LTC data (Figures 1b and 1c), the moving average can have large deviations from the mean, forming some kind of mountain-valley structure. The LTC lead to periods of apparent drift in sea level variations, which is random in nature, but may be incorrectly interpreted as a trend driven by external forcing. To illustrate this point, we have computed a cumulative distribution function of 10,000 surrogate data sets of centennial LTC time series trends with prescribed Hurst exponent *H* (Figure 1d) and with a standard deviation of 100 mm that is characteristic for monthly TG records. Figure 1d shows, for example, that there is a 90% chance of finding an apparent sea level trend of ±1.5 mm/yr in the record with $H = 0.9$ and ±0.5 mm/yr in that with $H = 0.7$. In the uncorrelated data, ($H = 0.5$) this stochastic trend is much smaller and varies between ±0.1 mm/yr (90% confidence).

Thus, adequate modeling of the observed sea level power law behavior is crucial for distinguishing externally driven trends from natural climate variability [*Lennartz and Bunde*, 2009, 2012; *Bunde and Lennartz*, 2012]. Inspection of the longest TG records worldwide demonstrated that the power law scaling exponent is a

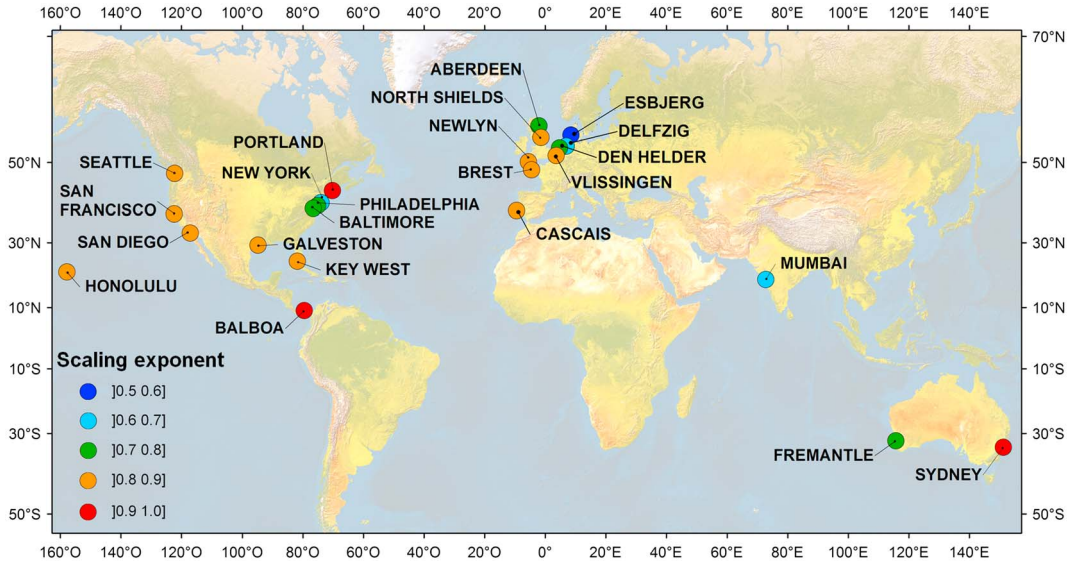

Figure 2. Location of the 23 historic tidal records and magnitude of the observed scaling exponent.

useful metric to characterize the sea level regional variability [*Beretta et al.*, 2005; *Barbosa et al.*, 2006, 2008; *Bos et al.*, 2013; *Becker et al.*, 2014; *Dangendorf et al.*, 2014a, 2015]. Moreover, several studies have previously demonstrated through other parameters (temperature, precipitation, water discharge…) the ability of this metric to characterize the stochastic variability of climate and to provide an important test of the validity of AOGCMs [*Bunde et al.*, 2001; *Govindan et al.*, 2001, 2002; *Vjushin et al.*, 2002; *Blender and Fraedrich*, 2003; *Blender et al.*, 2006; *Koutsoyiannis et al.*, 2008; *Rybski et al.*, 2008; *Kumar et al.*, 2013; *Bordbar et al.*, 2015]. By consequence, the main question that motivated this study was the following: Is the power law behavior observed in the tidal records also identifiable in the AOGCMs?

2. Data and Methods

We analyze 23 long-term monthly mean sea level TG records included in the Revised Local Reference data set of the Permanent Service for Mean Sea Level database [*Permanent Service for Mean Sea Level*, 2014; *Holgate et al.*, 2013]. We select TG records with at least 100 years of data, with exception of the Newlyn and Brest records (98 and 94 years, respectively), and with small gaps ($\leq$4 consecutive years). We excluded all TGs from the semienclosed seas, which are not properly represented in the coarse resolution global climate models. This selection finally gives 23 TGs listed in Table S1 in the supporting information and shown in Figure 2. The AOGCMs do not account for the direct effect of atmospheric pressure on sea level (the inverted barometer effect). Therefore, we have corrected all tide-gauge time series for the inverted barometer effect using the Hadley Center mean sea level pressure data set (4° × 4° 1850–2014, HadSLP2r [*Allan and Ansell*, 2006]) and selecting the closest grid point to each TG station. Finally, for all considered time series, the seasonal variations have been removed by subtracting the mean values for each calendar month.

We analyze the sea level variations from historical experiments driven by natural and anthropogenic forcings in 36 models contributed to the CMIP5 [*Taylor et al.*, 2012]. A single realization was selected in the models providing multiple realizations. The model variable used here is the SSH (CMIP5 variable *zos*). To obtain total sea level, SSH must be combined with global average thermosteric sea level change (CMIP5 variable *zostoga*). However, many models (15 among 36 models) do not include the *zostoga* variable to the CMIP5 archive. Therefore, in order to consider a maximum number of models, we have evaluated the relevance of adding the slowly varying global ocean thermal expansion to local sea level changes. The scaling exponents estimated from *zos* + *zostoga* data have been compared against those obtained only from *zos* data and no significant difference was found (see Figure S1 in the supporting information). The presence of LTC seemed to occur mainly in SSH, which include the regional variability of dynamic topography changes than in global average thermosteric component. For the purpose of the present work, we consider more relevant to include the highest number of models and we analyze below only the SSH variations stored as the *zos* variable. We

analyze the modeled SSH from: (1) the historical experiments (called historical runs hereinafter) driven by both time-dependent anthropogenic (greenhouse gas concentrations, aerosols, and ozone) and natural (solar and volcanic) forcings and (2) the experiments for the same period (called historicalNat runs) with only the time-dependent natural forcings corresponding to the Earth's climate without anthropogenic influences. Monthly SSH data from historical and historicalNat runs from climate models (listed in Table S2) were first interpolated bi-linearly onto the same regular $1° \times 1°$ grid. The closest grid point at each TG site was selected for comparison. These series were deseasonalized in the same way as the TGs and then used to estimate the scaling exponent over the TG time period.

In the following, we are interested in the dimensionless "relative" sea level trend defined as the ratio of Δ/σ_t, where Δ is the total sea level rise over the considered period and σ_t is the standard deviation around the regression line [*Lennartz and Bunde*, 2012]. For determining the scaling exponent α, we use the Detrended Fluctuation Analysis of order 2 (DFA2). DFA2 is a widely used approach for capturing the presence of LTC [*Peng et al.*, 1994; *Kantelhardt et al.*, 2001]. This method removes the influence of all linear trends. Therefore, the glacial isostatic adjustment effect on TG records and the possible drift in *zos* data [*Gupta et al.*, 2013] are directly removed by this method. In the following, we present briefly the main steps of the *n*-order DFA procedure for a record $X(i)$, $i = 1 \ldots L$. First, we determine the number of intervals of equal length $L_s = \lfloor L/s \rfloor$ and integrate the record: $y(k) = \sum_{k=1}^{L} X_k - \langle X \rangle$, where $\langle X \rangle$ is the data mean. Next, we divide the integrated time series into L_s nonoverlapping intervals. In each interval, we fit the integrated time series by using a *n*-order polynomial function, $p_v(k)$ in the *v*th window of size s ($v = 1, \ldots, L_s$), which is regarded as the local trend. In each interval, we subtract it to get the detrended fluctuations: $y_v(k) = y(k) - p_v(k)$. The variance of this integrated and detrended time series is calculated as: $F_v^2(s) = \frac{1}{s}\sum_{k(v)=1}^{s} y_v(k)^2$. This computation is repeated over all time scales to provide the fluctuation function: $F(s) = \sqrt{\frac{1}{L_s}\sum_{v=1}^{L_s} F_v^2(s)}$. The scaling exponent α is calculated as the slope of a straight line relating $ln(F(s))$ to $ln(s)$. A suitable 95% confidence interval for the scaling exponent α is given by two-tailed Student's *t* test. The exponent α corresponds to the Hurst exponent *H* when $0 < \alpha < 1$ [*Hurst et al.*, 1965; *Feder,* 1988]. Some TG records manifest, however, a scaling with $\alpha > 1$ [*Becker et al.*, 2014], indicating nonstationary long-term memory processes [*Beran*, 1994].

In our analysis, we chose sea level records longer than $L > 1200$ months because the error in estimation of α by DFA2 gets larger in the shorter series [*Kantelhardt et al.*, 2001]. Here we fitted α between scales $s = 60$ and $s = 180$ months. We skipped fitting at shorter scales to avoid the influence of short-range memory and the larger scales because of statistical fluctuations of the detrended fluctuation function on these scales.

3. Results

In order to compare scaling in the modeled and observed sea level variations, we used a simple binary score: If, at a 99% confidence level, the scaling exponent of the modeled sea level series is not statistically different from that of the tidal record, then the score is set to 1 (a successful model); otherwise, it is set to zero. We employed Welch's *t* test, two-sample *t* test for unequal variance [*Welch*, 1938], to identify the significant differences between the scaling exponents α (see section 2). Figure 3 presents the AOGCM scores for the 99% confidence interval: The colored squares correspond to successful matches; i.e., the scaling exponents in the modeled and observed sea level fluctuations are statistically undistinguishable, and the white squares indicate the cases when the scaling exponents in model simulations are statistically different from the observations. The colors of Figure 3 columns vary to highlight different oceanic regions. A row with no white squares in Figure 3 would represent a model with good performance, while an "easy-to-predict" TG record, i.e., one whose scaling is reproduced successfully by all models, would be recognizable as a fully colored column. The histogram on the right in Figure 3 displays, for each model, the number of TGs where the observed and modeled scaling exponents α are equal at a 99% significance level. The histogram at bottom of Figure 3 quantifies how many models correctly estimate the scaling exponent α at each TG. An overall view of Figure 3 shows no perfect model, neither an "easy-to-predict" TG record: Although some models perform certainly better than others, their skill varies from one region to another. The first result, after examining the distribution of the scores, is that there is no systematic difference between the results obtained with the historicalNat forcing and those from the historical runs. We cannot conclude, however, that the impact of

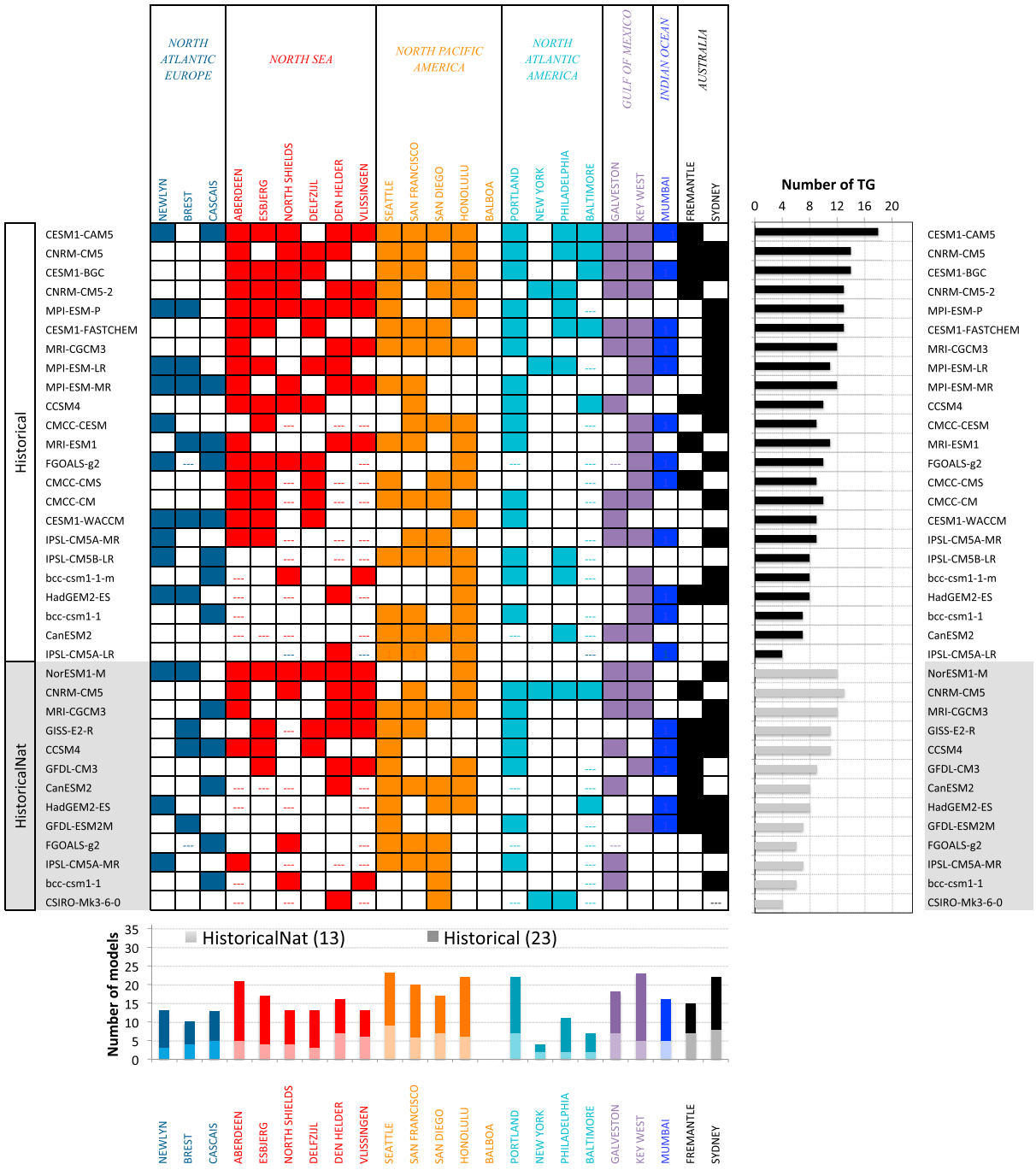

Figure 3. Comparison of observed and model scaling exponents. The colored squares mark statistically undistinguishable (at 99%) scaling exponents in the modeled and observed sea level fluctuations, and the white squares to the scaling exponents statistically different between observations and models. A hyphen (-) means that comparison is not possible.

anthropogenic forcing on the scaling exponent is negligible: perhaps, it is hidden by other sources of model uncertainties.

Figure 3 provides insights into models accuracy but cannot tell whether the spread in the modeled scaling exponent α is symmetric or there are some biases due to systematic errors/inadequate parameterizations in the climate models. To evaluate the possible biases, Figure 4 assembles, for every tidal station, scaling exponents obtained from all the models versus the observed one (indicated by a red line). Strikingly, the

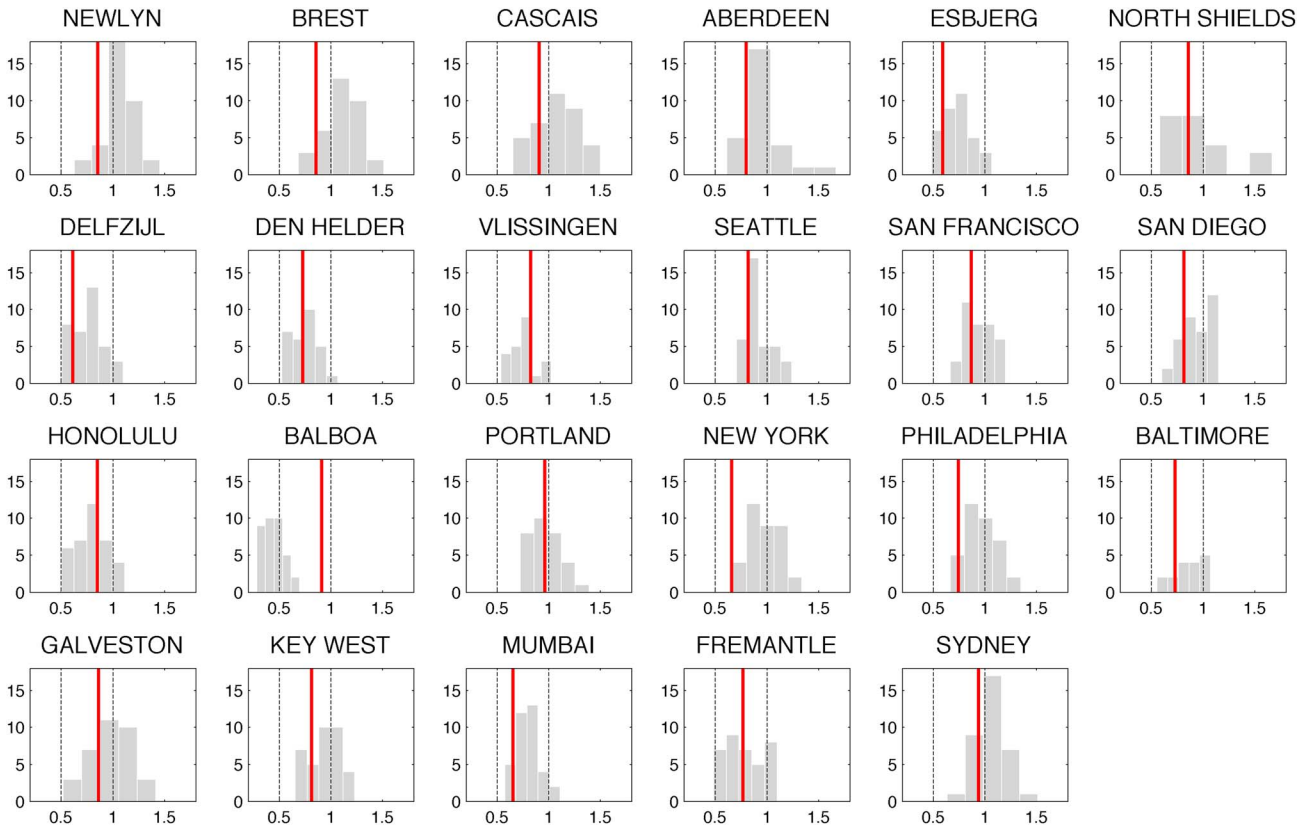

Figure 4. Estimate of the scaling exponent by the models. The grey bars are the scaling exponents predicted by the AOGCMs, and the red line is the scaling exponent observed in TG record.

scaling exponents of the Newlyn, Brest, and Cascais tidal records (~0.9), all from the Eastern North Atlantic coast, are significantly overestimated by the AOGCMs. The bias is less evident in the North Sea, at Aberdeen, Esbjerg, and North Shields as well as at Delfzijl and Den Helder, and it even changes the sign at Vlissingen where the models underestimate the scaling exponent α. However, some caution is required in interpreting the TG record at Vlissingen as its trend is not in agreement with that in the neighboring TG records [*Wahl et al.*, 2013]. It is instructive to look at the long-term correlations predicted by the AOGCMs at the Western coast of the North Atlantic, where at all TGs, except Portland, the scaling exponent is significantly overestimated as well (see New York, Philadelphia, and Baltimore). The magnitude of the scaling exponent in the Portland tidal record is about 0.9, larger than that at New York, Philadelphia, and Baltimore, where it is about 0.7. The bias between the predicted and observed scaling exponent is less evident in the Gulf of Mexico although a slight overprediction can be evoked at Key West and Galveston. Inspecting the North Pacific, tidal records do not show a regular overestimation of the scaling exponents as in the North Atlantic, although at San Diego the scaling exponent is clearly overestimated by the AOGCMs. A striking misfit is detected at Balboa where 25 AOGCMs among 36 (70%) predict white-noise or even antipersistent ($0 < \alpha < 0.5$) sea level fluctuations. The Balboa TG is situated on the west coast of Panama, and its monthly data were shown to agree with those from the neighboring stations (http://store.pangaea.de/Projects/WOCE/SeaLevel_rqds/Balboa.txt). However, some differences with the open-ocean sea level were recently pointed through comparison of the Balboa TG to the satellite altimetry measurements [*Etcheverry et al.*, 2015]. We suppose that underestimation of scaling exponent at Balboa is due mostly to the coarse resolution of the AOGCMs that cannot resolve the particularities of the coastal sea level changes. By consequence, the modeled sea level at Balboa is dominated by the oceanic signal that is, in turn, affected by the El Nino/Southern Oscillation events. As the El Nino/Southern Oscillation event was reported to manifest an antipersistent behavior ($\alpha < 0.5$) [*Ausloos and Ivanova*, 2001], the modeled scaling exponent at Balboa is lower than the observed one. It is worthy of noting that if the models cannot resolve the sea level variability

induced by the shelf waves the sea level variations can be significantly mispredicted over long distances on the continental shelf [*Clarke*, 1977; *Calafat et al.*, 2012; *Andres et al.*, 2013; *Dangendorf et al.*, 2014b].

It is interesting that there is no noticeable bias between the observed and predicted scaling exponents at Honolulu although the intermodel spread is still large. The AOGCMs show rather different performances in predicting two Australian records. The majority of models match quite closely the observed scaling exponent (0.9) at Sydney, but there are just several models that succeed to approach the observed scaling exponent (0.8) at Fremantle. And, finally, the scaling in the single historical sea level record in the Indian Ocean, at Mumbai (0.7), seems, again, to be overestimated by the AOGCMs ensemble. In addition, it is important to note that many AOGCMs predict scaling exponents superior to 1 that implies nonstationary behavior of the SSH fluctuations. This is especially remarkable in the Eastern North Atlantic, where 70% of the predicted scaling exponents are larger than 1. Similarly, on average, 35% of predicted scaling exponents are larger than 1 along the Atlantic coast of North America (Baltimore is not included) and as well as 35% of scaling exponents in the Eastern North Pacific (Balboa and Honolulu are not included). Looking overall, the long-term correlations seem to be overestimated by the AOGCMs across all oceans and particularly, in the North Atlantic. There are multiple reasons for systematic differences across the CMIP5 models in their representation of North Atlantic decadal variability [*Menary et al.*, 2015]. An enhanced spatial resolution seems to be crucial for the next generations of the AOGCMs as it is necessary both for resolving the shelf processes and the deep ocean internal variability [*Penduff et al.*, 2011; *Sérazin et al.*, 2015].

What the consequences can overestimating of scaling exponents have for climate predictions? In order to illustrate this point let us consider, for example, sea level fluctuations at the New York City. The New York TG record is characterized by $\alpha_{TG} = 0.7$, while the modeled sea level has $\alpha_{Model} > 0.9$. *Little et al.* [2015] discussed the sea level change projections from CMIP5 AOGCMs at New York City in 2090. These projections give a sea level rise between 33 cm and 56 cm in 2090 (see Figure 10 from *Little et al.* [2015] for more details). We can apply Lennartz-Bunde statistics (see Figure 8b from *Lennartz and Bunde* [2012]) to estimate the consequences of overpredicting the scaling exponent in New York. Over the century-long period, the sea level fluctuations observed from the TG record at New York have $\alpha_{TG} = 0.7$ and a standard deviation of $\sigma_{TG} = 57$ mm. If these parameters stay unchanged till 2090, it means that with 95% confidence, the sea level can drift away from its *externally driven* rise by up to 5 cm (15% or 9% of 33 or 56 cm, respectively, due to the total sea level change at the end of 2090). This drift is solely due to the natural sea level variability not to the presence of externally driven sea level trend. In contrast, the naturally driven sea level change for example can reach 19 cm (95% confidence) in 2090 in CESM1-WACCM (Community Earth System Model version 1-Whole Atmosphere Community Climate Model) because its modeled sea level fluctuations in New York have $\alpha_{Model} = 1.3$ and a standard deviation of $\sigma_{Model} = 25$ mm. The natural variability in this model is about 58% or 34% of 33 or 56 cm, respectively, corresponding to the total sea level change at the end of 2090. As a consequence, a sea level change between 5 cm and 19 cm is unlikely of natural origin in the first case ($\alpha = 0.7$), while in the second case ($\alpha = 1.3$) a natural origin cannot be excluded. Thus, overestimating the scaling exponents can mask the part of the externally driven relative sea level trend, in particular the anthropogenic footprint, in the sea level projections for the 21st century.

Figures 3 and 4 show also that the best performance was obtained in the National Center for Atmospheric Research CESM1-CAM5 historical (Community Earth System Model-Community Atmosphere Model version 5) that simulated successfully the scaling exponent in 18 TG records among the 23. A second group including the CNRM-CM5 historical (National Centre for Meteorological Research-Climate Model) and CNRM-CM5-2 historical [*Voldoire et al.*, 2012] successfully provided the scaling exponent in 14 and 13 TG records out of 23, respectively. Both models performed very well in The North Sea, the Eastern North Pacific, and the Gulf of Mexico. Nevertheless, the models performance is not as good in the North Atlantic. By overestimating the long-term persistence, the AOGCMs introduce more substantial long-term variations that can mask relative the external trends and, by consequence, underestimate sea level change due to external forcing in the 21st century projections. It is interesting to note that the three best-performing models have the highest spatial resolution: $<1.5°$ in the atmospheric model (AGCM) and $\leq 1°$ in the oceanic model (OGCM) (see Table S2).

4. Conclusions

We employed a scaling exponent as a metric for assessing the performance of AOGMC in modeling the complexity of sea level fluctuations. Comparison of the scaling behavior measured in the century-long TG records

with that in modeled SSH variations showed a large spread in performance among the 36 CMIP5 AOGCM models. The best fit ting simulation of the SSH scaling was provided by CESM1-CAM5 driven by historical forcing: It reproduced the observed scaling at 18 tidal stations among 23. No systematic difference in predicting skills was found between the AOGCM runs driven by historical or natural-only forcing. There is apparently a tendency in the ensemble of the CMIP5 models to overestimate the scaling of sea level fluctuations especially in the North Atlantic, both in the East (Newlyn, Brest, and Cascais) and in the West (New York, Baltimore, and Philadelphia). By consequence, much care should be taken in applying the regional projections issued by an AOGCM that fails to reproduce the observed sea level scaling in the past.

Acknowledgments
We acknowledge the Permanent Service for Mean Sea Level, Proudman Oceanographic Laboratory, UK, for making available the tide-gauge records. We thank the Met Office Hadley Center for providing the Hadley Centre's monthly historical mean sea level pressure data set (online at http://www.metoffice.gov.uk/hadobs/hadslp2/). We acknowledge also the World Climate Research Program's Working Group on Coupled Modelling, and we thank the climate modeling groups (listed in Table S1) for producing and making available their model output. The TOSCA/CNES program supported this study.

References

Agnew, D. C. (1992), The time-domain behavior of power-law noises, *Geophys. Res. Lett.*, *19*(4), 333–336.
Allan, R., and T. Ansell (2006), A new globally complete monthly historical gridded mean sea level pressure dataset (HadSLP2): 1850–2004, *J. Clim.*, *19*(22), 5816–5842, doi:10.1175/JCLI3937.1.
Andres, M., G. G. Gawarkiewicz, and J. M. Toole (2013), Interannual sea level variability in the western North Atlantic: Regional forcing and remote response, *Geophys. Res. Lett.*, *40*, 5915–5919, doi:10.1002/2013GL058013.
Ausloos, M., and K. Ivanova (2001), Power-law correlations in the southern-oscillation-index fluctuations characterizing El Niño, *Phys. Rev. E*, *63*(4), 047201.
Barbosa, S. M., M. J. Fernandes, and M. E. Silva (2006), Long-range dependence in North Atlantic sea level, *Physica A*, *371*(2), 725–731.
Barbosa, S. M., M. E. Silva, and M. J. Fernandes (2008), Time series analysis of sea-level records: Characterising long-term variability, in *Nonlinear Time Series Analysis in the Geosciences*, pp. 157–173, Springer, Berlin.
Becker, M., B. Meyssignac, C. Letetrel, W. Llovel, A. Cazenave, and T. Delcroix (2012), Sea level variations at tropical Pacific islands since 1950, *Global Planet. Change*, *80*, 85–98.
Becker, M., M. Karpytchev, and S. Lennartz-Sassinek (2014), Long-term sea level trends: Natural or anthropogenic?, *Geophys. Res. Lett.*, *41*, 5571–5580, doi:10.1002/2014GL061027.
Beran, J. (1994), *Statistics for Long-Memory Processes*, CRC Press, Boca Raton.
Beretta, A., H. E. Roman, F. Raicich, and F. Crisciani (2005), Long-time correlations of sea-level and local atmospheric pressure fluctuations at Trieste, *Physica A*, *347*, 695–703.
Bilbao, R. A., J. M. Gregory, and N. Bouttes (2015), Analysis of the regional pattern of sea level change due to ocean dynamics and density change for 1993–2099 in observations and CMIP5 AOGCMs, *Clim. Dyn.*, 1–20.
Blender, R., and K. Fraedrich (2003), Long time memory in global warming simulations, *Geophys. Res. Lett.*, *30*(14), 1769, doi:10.1029/2003GL017666.
Blender, R., K. Fraedrich, and B. Hunt (2006), Millennial climate variability: GCM-simulation and Greenland ice cores, *Geophys. Res. Lett.*, *33*, L04710, doi:10.1029/2005GL024919.
Bordbar, M. H., T. Martin, M. Latif, and W. Park (2015), Effects of long-term variability on projections of twenty-first century dynamic sea level, *Nat. Clim. Change*, *5*(4), 343–347, doi:10.1038/nclimate2569.
Bos, M. S., S. D. P. Williams, I. B. Araújo, and L. Bastos (2013), The effect of temporal correlated noise on the sea level rate and acceleration uncertainty, *Geophys. J. Int*, doi:10.1093/gji/ggt481.
Bunde, A., and S. Lennartz (2012), Long-term correlations in Earth sciences, *Acta Geophys.*, *60*(3), 562–588.
Bunde, A., S. Havlin, E. Koscielny-Bunde, and H.-J. Schellnhuber (2001), Long term persistence in the atmosphere: Global laws and tests of climate models, *Physica A*, *302*(1), 255–267.
Calafat, F. M., D. P. Chambers, and M. N. Tsimplis (2012), Mechanisms of decadal sea level variability in the eastern North Atlantic and the Mediterranean Sea, *J. Geophys. Res.*, *117*, C09022, doi:10.1029/2012JC008285.
Cazenave, A., and W. Llovel (2010), Contemporary sea level rise, *Annu. Rev. Mar. Sci.*, *2*, 145–173.
Church, J. A., N. J. White, R. Coleman, K. Lambeck, and J. X. Mitrovica (2004), Estimates of the regional distribution of sea level rise over the 1950–2000 period, *J. Clim.*, *17*(13).
Clarke, A. J. (1977), Observational and numerical evidence for wind-forced coastal trapped long waves, *J. Phys. Oceanogr.*, *7*(2), 231–247.
Dangendorf, S., D. Rybski, C. Mudersbach, A. Müller, E. Kaufmann, E. Zorita, and J. Jensen (2014a), Evidence for long-term memory in sea level, *Geophys. Res. Lett.*, *41*, 5530–5537, doi:10.1002/2014GL060538.
Dangendorf, S., F. M. Calafat, A. Arns, T. Wahl, I. D. Haigh, and J. Jensen (2014b), Mean sea level variability in the North Sea: Processes and implications, *J. Geophys. Res. Oceans*, *119*, 6820–6841, doi:10.1002/2014JC009901.
Dangendorf, S., M. Marcos, A. Müller, E. Zorita, R. Riva, K. Berk, and J. Jensen (2015), Detecting anthropogenic footprints in sea level rise, *Nat. Commun.*, *6*, doi:10.1038/ncomms8849.
Etcheverry, L. R., M. Saraceno, A. R. Piola, G. Valladeau, and O. O. Möller (2015), A comparison of the annual cycle of sea level in coastal areas from gridded satellite altimetry and tide gauges, *Cont. Shelf Res.*, *92*, 87–97.
Feder, J. (1988), *Fractals, 1988*, Plenum Press, New York.
Govindan, R. B., D. Vjushin, S. Brenner, A. Bunde, S. Havlin, and H.-J. Schellnhuber (2001), Long-range correlations and trends in global climate models: Comparison with real data, *Physica A*, *294*(1), 239–248.
Govindan, R. B., D. Vyushin, A. Bunde, S. Brenner, S. Havlin, and H.-J. Schellnhuber (2002), Global climate models violate scaling of the observed atmospheric variability, *Phys. Rev. Lett.*, *89*(2), 028501.
Griffies, S. M., and R. J. Greatbatch (2012), Physical processes that impact the evolution of global mean sea level in ocean climate models, *Ocean Model.*, *51*, 37–72, doi:10.1016/j.ocemod.2012.04.003.
Gupta, A. S., N. C. Jourdain, J. N. Brown, and D. Monselesan (2013), Climate drift in the CMIP5 models*, *J. Clim.*, *26*(21), 8597–8615.
Holgate, S. J., A. Matthews, P. L. Woodworth, L. J. Rickards, M. E. Tamisiea, E. Bradshaw, P. R. Foden, K. M. Gordon, S. Jevrejeva, and J. Pugh (2013), New data systems and products at the Permanent Service for Mean Sea Level, *J. Coast. Res.*, *288*, 493–504, doi:10.2112/JCOASTRES-D-12-00175.1.
Hughes, C. W., and S. D. Williams (2010), The color of sea level: Importance of spatial variations in spectral shape for assessing the significance of trends, *J. Geophys. Res.*, *115*, C10048, doi:10.1029/2010JC006102.
Hurst, H. E., R. P. Black, and Y. M. Simaika (1965), *Long-term Storage: An Experimental Study*, Constable, London.

Jevrejeva, S., A. Grinsted, J. C. Moore, and S. Holgate (2006), Nonlinear trends and multiyear cycles in sea level records, *J. Geophys. Res.*, *111*, C09012, doi:10.1029/2005JC003229.

Kantelhardt, J. W., E. Koscielny-Bunde, H. H. Rego, S. Havlin, and A. Bunde (2001), Detecting long-range correlations with detrended fluctuation analysis, *Physica A*, *295*(3), 441–454.

Koutsoyiannis, D., A. Efstratiadis, N. Mamassis, and A. Christofides (2008), On the credibility of climate predictions, *Hydrol. Sci. J.*, *53*(4), 671–684.

Kumar, S., V. Merwade, J. L. Kinter III, and D. Niyogi (2013), Evaluation of temperature and precipitation trends and long-term persistence in CMIP5 twentieth-century climate simulations, *J. Clim.*, *26*(12), 4168–4185.

Landerer, F. W., P. J. Gleckler, and T. Lee (2014), Evaluation of CMIP5 dynamic sea surface height multi-model simulations against satellite observations, *Clim. Dyn.*, *43*(5–6), 1271–1283.

Lennartz, S., and A. Bunde (2009), Trend evaluation in records with long-term memory: Application to global warming, *Geophys. Res. Lett.*, *36*, L16706, doi:10.1029/2009GL039516.

Lennartz, S., and A. Bunde (2012), On the estimation of natural and anthropogenic trends in climate records, *Geophys. Monogr. Ser.*, *196*, 177–189.

Little, C. M., R. M. Horton, R. E. Kopp, M. Oppenheimer, and S. Yip (2015), Uncertainty in twenty-first-century CMIP5 sea level projections, *J. Clim.*, *28*(2), 838–852.

Mandelbrot, B. B., and J. R. Wallis (1968), Noah, Joseph, and operational hydrology, *Water Resour. Res.*, *4*(5), 909–918, doi:10.1029/WR004i005p00909.

Mandelbrot, B. B., and J. R. Wallis (1969), Some long-run properties of geophysical records, *Water Resour. Res.*, *5*(2), 321–340, doi:10.1029/WR005i002p00321.

Menary, M. B., D. L. Hodson, J. I. Robson, R. T. Sutton, R. A. Wood, and J. A. Hunt (2015), Exploring the impact of CMIP5 model biases on the simulation of North Atlantic decadal variability, *Geophys. Res. Lett.*, *42*, 5926–5934, doi:10.1002/2015GL064360.

Mitchum, G. T., R. S. Nerem, M. A. Merrifield, and W. R. Gehrels (2010), Modern sea-level-change estimates, in *Understanding Sea-Level Rise and Variability*, pp. 122–142, Wiley Blackwell, Chichester, U. K.

Nerem, R. S., D. P. Chambers, C. Choe, and G. T. Mitchum (2010), Estimating mean sea level change from the TOPEX and Jason altimeter missions, *Mar. Geod.*, *33*(S1), 435–446.

Penduff, T., M. Juza, B. Barnier, J. Zika, W. K. Dewar, A.-M. Treguier, J.-M. Molines, and N. Audiffren (2011), Sea level expression of intrinsic and forced ocean variabilities at interannual time scales, *J. Clim.*, *24*(21), 5652–5670.

Peng, C.-K., S. V. Buldyrev, S. Havlin, M. Simons, H. E. Stanley, and A. L. Goldberger (1994), Mosaic organization of DNA nucleotides, *Phys. Rev. E*, *49*(2), 1685.

PSMSL (2014), Permanent Service for Mean Sea Level (PSMSL), "Tide Gauge Data." [Available at http://www.psmsl.org/data/obtaining/, accessed on 23 Jun 2014.]

Rybski, D., and A. Bunde (2009), On the detection of trends in long-term correlated records, *Physica A*, *388*(8), 1687–1695.

Rybski, D., A. Bunde, and H. Von Storch (2008), Long-term memory in 1000-year simulated temperature records, *J. Geophys. Res.*, *113*, D02106, doi:10.1029/2007JD008568.

Sérazin, G., T. Penduff, S. Grégorio, B. Barnier, J.-M. Molines, and L. Terray (2015), Intrinsic variability of sea level from global ocean simulations: Spatiotemporal scales, *J. Clim.*, *28*(10), 4279–4292.

Stammer, D., A. Cazenave, R. M. Ponte, and M. E. Tamisiea (2013), Causes for contemporary regional sea level changes, *Annu. Rev. Mar. Sci.*, *5*(1), 21–46, doi:10.1146/annurev-marine-121211-172406.

Taylor, K. E., R. J. Stouffer, and G. A. Meehl (2012), An overview of CMIP5 and the experiment design, *Bull. Am. Meteorol. Soc.*, *93*(4), 485–498.

Vjushin, D., R. B. Govindan, S. Brenner, A. Bunde, S. Havlin, and H. J. Schellnhuber (2002), Lack of scaling in global climate models, *J. Phys. Condens. Matter*, *14*(9), 2275.

Voldoire, A., et al. (2012), The CNRM-CM5.1 global climate model: Description and basic evaluation, *Clim. Dyn.*, *40*(9–10), 2091–2121, doi:10.1007/s00382-011-1259-y.

Wahl, T., I. D. Haigh, P. L. Woodworth, F. Albrecht, D. Dillingh, J. Jensen, R. J. Nicholls, R. Weisse, and G. Wöppelmann (2013), Observed mean sea level changes around the North Sea coastline from 1800 to present, *Earth Sci. Rev.*, *124*, 51–67.

Welch, B. L. (1938), The significance of the difference between two means when the population variances are unequal, *Biometrika*, *29*(3/4), 350–362.